TRENDS IN SCIENCES 2025; 22(6): 9657 RESEARCH ARTICLE
https://doi.org/10.48048/tis.2025.9657

Study of Selectivity Anionic Dye Removal and Sustainable Regeneration of Hydrochar from *Spirogyra* sp. Algae Biomass

Muhammad Badaruddin[1], Laila Hanum[3], Elda Melwita[2], Sahrul Wibiyan[2,4], Alfan Wijaya[1], Nur Ahmad[4,5] and Aldes Lesbani[2,4,*]

[1]*Doctoral Program of Environmental Science, Postgraduate Program, Universitas Sriwijaya, South Sumatera 30139, Indonesia*
[2]*Master Program of Materials Science, Graduate School, Universitas Sriwijaya, South Sumatera 30139, Indonesia*
[3]*Biology Department, Faculty of Mathematics and Natural Sciences, Universitas Sriwijaya, South Sumatera 30662, Indonesia*
[4]*Research Center of Inorganic Materials and Coordination Complexes, Universitas Sriwijaya, South Sumatera 30139, Indonesia*
[5]*Doctoral Program of Natural Science, Graduate School Faculty of Mathematics and Natural Sciences, Universitas Sriwijaya, South Sumatera 30139, Indonesia*

([*]Corresponding author's e-mail: aldeslesbani@pps.unsri.ac.id)

Received: 30 December 2024, Revised: 4 February 2025, Accepted: 11 February 2025, Published: 1 May 2025

Abstract

This study investigates the synthesis of hydrochar from *Spirogyra* sp. algae biomass and its selective adsorption performance for anionic dyes. The hydrochar (SpiHC) was prepared via hydrothermal carbonization and characterized using XRD, FTIR, and BET analysis, revealing a significant increase in surface area (5.369 m^2/g) and the development of a more ordered carbon structure. Selectivity studies showed that direct yellow (DY) exhibited the highest adsorption efficiency, with 62.07 % on SpiHC compared to 54.02 % on unmodified *Spirogyra* sp. (Spi). Adsorption experiments demonstrated optimal conditions at pH 6 and fit better with the pseudo-second-order kinetic model. Freundlich isotherm analysis indicated improved adsorption capacity and surface affinity of SpiHC. Thermodynamic parameters confirmed the endothermic and spontaneous nature of the adsorption process, with SpiHC showing higher adsorption affinity than Spi. Regeneration studies revealed that SpiHC retained 67.11 % adsorption efficiency after 4 cycles, highlighting its superior stability and reusability compared to Spi. These findings demonstrate the potential of *Spirogyra*-derived hydrochar as a sustainable adsorbent for water treatment applications.

Keywords: *Spirogyra* sp., Hydrochar, Selectivity, Regeneration, Anionic dye

Introduction

The presence of industrial waste containing dyes represents a considerable environmental challenge [1]. The primary origin of this effluent is attributed to multiple industrial sectors, including textile, leather, and printing, which utilize a range of synthetic dyes [2], [3]. Anionic dyes, including direct yellow, congo red, and direct green, represent a category of dyes frequently encountered in industrial wastewater effluents [4], [5]. The utilization of these dyes, although advantageous for industrial applications, may pose significant risks to environmental integrity and human health [6]. Anionic dyes exhibit a notable stability that renders them resistant to natural degradation processes [7]. This characteristic contributes to their detrimental accumulation within ecosystems, leading to significant contamination of both aquatic and terrestrial environments.

Effective solutions are required to diminish the content of dyes in wastewater to address this issue. A prevalent technique is adsorption, in which adsorbent materials attract and bind color molecules [8]. Nevertheless, due to the variety of dye types, it is essential to enhance the selectivity of adsorbents for particular dyes [9]. This selectivity is essential to guarantee that the adsorbent can effectively adsorb the target dye, for example direct yellow in anionic dyes, without interference from other dyes present in the effluent [10].

Numerous materials have been employed in adsorption processes for the treatment of dye effluents, including activated carbon, zeolites, and biomass-derived materials [11], [12]. Nonetheless, numerous materials exhibit constraints regarding their efficiency and associated costs. Hydrochar, a product of biomass carbonization achieved via a hydrothermal process, is gaining recognition as a promising alternative [13]. Hydrochar exhibits significant adsorption capacity attributed to its unique structural configuration and the presence of specific functional groups [14]. *Spirogyra* sp. algae represents a promising biomass source for hydrochar production, characterized by its richness in organic compounds and its potential applicability in the adsorption of anionic dyes [15].

The hydrochar derived from *Spirogyra sp*. exhibits a range of functional groups that may improve its capacity for the adsorption of anionic dyes. Functional groups including hydroxyl (-OH), carboxylate (-COOH), and amine (-NH_2) exhibit interactions with the negatively charged ions present in anionic dyes [16]. The electrostatic interactions and the establishment of hydrogen bonds with these functional groups facilitate the selective and efficient adsorption of dyes by the hydrochar [17]. The pivot structure of the hydrochar significantly enhances its surface area, thereby promoting an increased adsorption capacity [18].

This study investigates the application of hydrochar derived from *Spirogyra* sp. as an adsorbent for anionic dyes, particularly highlighting its selectivity towards Direct Yellow. This research presents a significant advantage through the employment of *Spirogyra sp*. algae, a subject that has not been extensively investigated in the context of dye adsorption. Furthermore, it adopts a selective methodology targeting specific anionic dyes. The characterization of the adsorbent material was conducted utilizing a range of techniques, including X-ray diffraction (XRD), Fourier-transform infrared spectroscopy (FTIR), and Brunauer-Emmett-Teller (BET) analysis, to assess the physical and chemical properties of the hydrochar from *Spirogyra sp*. The kinetics, isotherm, thermodynamics, and regeneration parameters of the material were systematically analyzed to evaluate the performance of the adsorbent in the adsorption process, as well as its sustainability in practical applications.

Materials and methods

Chemical and instrumental

The chemicals used in this study were analytical-grade reagents, including sodium hydroxide (NaOH, ≥ 98 % purity, Merck), hydrochloric acid (HCl, 37 % w/w, Sigma-Aldrich), and distilled water (H_2O). The anionic dyes used for adsorption experiments included direct yellow, methyl orange, congo red, methyl red, and direct green, all obtained from Sigma-Aldrich. The *Spirogyra* sp. algae sample was collected from Lebung Jangkar Village, Pemulutan District, Ogan Ilir Regency, South Sumatra Province (coordinates: –3.113052, 104.786218 °).

The experimental setup involved standard laboratory glassware along with various analytical instruments. A hydrothermal stainless-steel autoclave (Toption, 100 mL capacity) was used for material synthesis. A microscope was employed for preliminary morphological analysis of the algae sample. The crystalline structure of the synthesized material was analyzed using X-ray Diffraction (XRD, Rigaku MiniFlex600) with Cu-Kα radiation (λ = 1.5406 Å) at 30 kV and 10 mA, scanning over a range of 2θ = 5 - 90 °. Fourier Transform Infrared Spectroscopy (FTIR, Shimadzu Prestige-21) was utilized to identify functional groups in the sample, with spectra recorded in the range of 4,000 - 400 cm^{-1}. The specific surface area, pore size, and volume were determined using a Brunauer-Emmett-Teller (BET) surface area analyzer (Quantachrome NovaWin) through N_2 adsorption-desorption isotherms at 77 K. The adsorption efficiency of the material for different dyes was assessed using an ultraviolet-visible (UV-Vis) spectrophotometer (EMC-18PC-UV), measuring absorbance in the 200 - 800 nm range at the characteristic wavelengths of each dye.

Algae *Spirogyra sp.* preparation

The *Spirogyra* sp. algae were thoroughly washed with distilled water, identified under a microscope, and then cut into small pieces. The pieces were dried in an oven at 100 °C until fully dried, after which they were crushed and sieved through a 100 mesh sieve. The resulting materials were characterized using XRD, FT-IR, and BET analysis.

Algae *Spirogyra sp.* hydrothermal carbonization

A total of 2.5 g of *Spirogyra* sp. algae preparation was added to 50 mL of distilled water and placed into a 100 mL hydrothermal stainless-steel autoclave. The autoclave was then placed in an oven at 150 °C for 12 h, after which it was cooled to room temperature, washed with distilled water, and dried in the oven at 105 °C for 24 h. The hydrochar material obtained was ground using a mortar, sieved through a 100 mesh sieve, and subsequently characterized by XRD, FT-IR, and BET analysis.

Determination of pHpzc (point zero charge) on adsorbent material

The pHpzc was determined by adding 0.02 g of each adsorbent to 20 mL of 0.1 M NaCl solution, which was adjusted to various pH values of 2, 3, 4, 5, 6, 7, 8, 9, 10, and 11. The pH of the NaCl solution was adjusted using 0.1 M NaOH and HCl solutions. The mixture was stirred for 24 h, then filtered. The final pH of the filtrate was measured using a pH meter, and a graph was plotted showing the relationship between the initial and final pH values.

Anionic dye selectivity

Anionic dye solutions (direct yellow, methyl orange, congo red, methyl red, and direct green) with absorbance values measured at 0.600 nm were prepared by combining 10 mL of each dye in a beaker. Then, 0.05 g of adsorbent was added to the dye mixture and stirred for 60 min. Wavelength measurements were taken using a UV-visible spectrophotometer. An adsorption study was performed on the selected anionic dyes.

Adsorption procedure

The adsorption process was conducted by varying parameters such as pH, contact time, dye concentration, and temperature to identify the optimal conditions for adsorbing direct yellow dye. pH variation was performed to determine the best adsorption conditions across a range from acidic to alkaline pH (pH 2 to pH 11) using NaOH and HCl. For this, 20 mL of direct yellow dye solution at a concentration of 30 mg/L was used. The initial absorbance was measured using a UV-Vis spectrophotometer. Then, 0.02 g of adsorbent was added, and the mixture was stirred for 2 h, after which the final absorbance was measured. Time variation experiments were carried out to find the optimal adsorption time, ranging from 5 to 210 min, with absorbance measured at each time point. The effect of concentration was assessed by adding 0.02 g of adsorbent to 20 mL of direct yellow dye solutions at concentrations of 10, 20, 30, and 40 mg/L, and the effect of temperature was analyzed at 30, 40, 50, and 60 °C. The solution was stirred for the optimal time, then separated, and the final absorbance was measured.

Reuse of regeneration adsorbent

A 25 mL solution of direct yellow dye at a concentration of 40 mg/L was placed into a beaker, and the pH of the solution was adjusted to the optimal pH. Then, 0.025 g of adsorbent was added. The mixture was stirred using a magnetic stirrer for the optimal adsorption time. Afterward, the adsorbent and adsorbate were separated. The filtrate, containing the adsorbate, was measured for absorbance using a UV-Vis spectrophotometer. The adsorbent was then washed with distilled water and desorbed using an ultrasonic device. After drying, the adsorbent was prepared for reuse in the next adsorption cycle, following the same procedure as the initial adsorption.

Results and discussion

Material characterization

XRD analysis

The primary peaks characterizing the Spi and SpiHC materials, as displayed in **Figure 1(a)**, are observed at 2θ values of approximately around 23, 26, 29, 36, 43, 47, 57, 61, and 65 °. These peaks correspond to the JCPDS data (01-086-2334), confirming that the material exhibits a phase comparable to calcium carbonate ($CaCO_3$) [19]. In the SpiHC material, a slight shift in the 2θ values is observed, along with the appearance of a new peak at approximately 16 °, which

is attributed to an increased ratio and the development of a more orderly carbon structure. This signifies the successful synthesis of hydrochar.

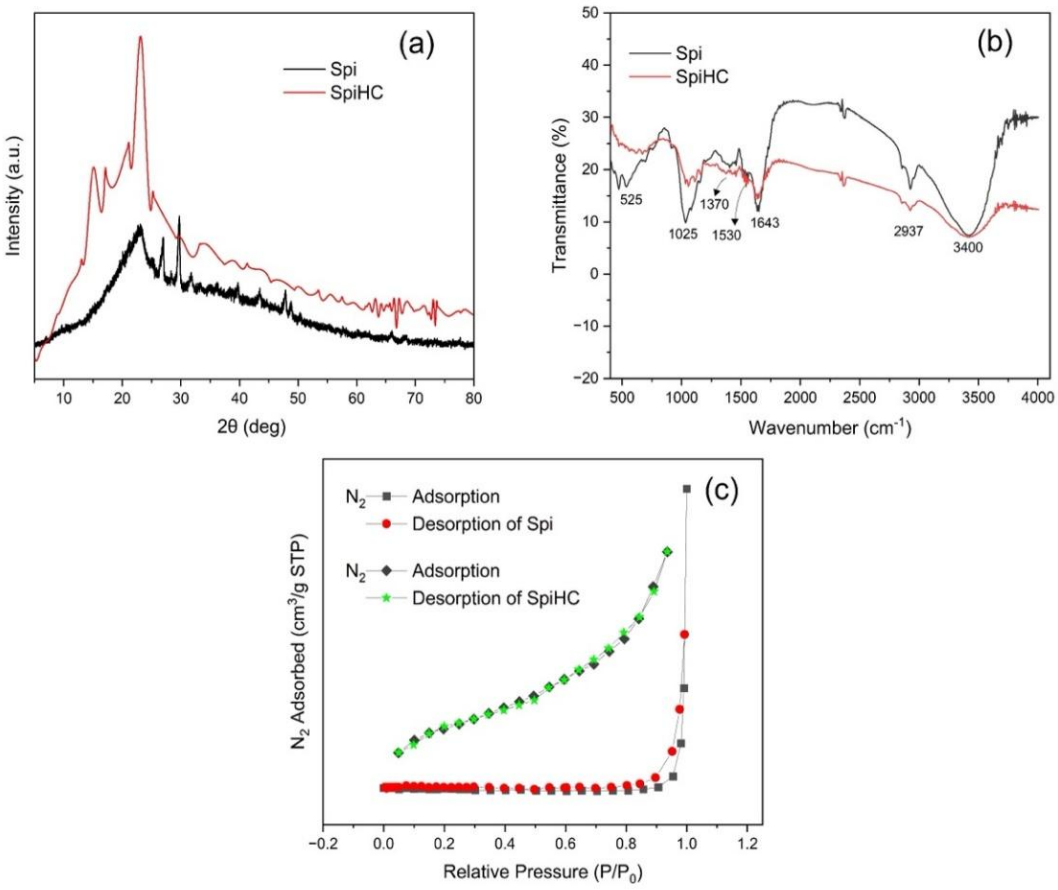

Figure 1 The XRD Pattern (a), FTIR Spectra (b) and BET N_2 Adsorption-Desorption (c) of Spi and SpiHC.

FTIR analysis

The FTIR analysis of Spi and SpiHC materials is shown in **Figure 1(b)**. The peak at 3,400 cm^{-1} is identified as the O-H stretching and N-H groups present in the material. Carboxyl and phenolic groups are detected at the peak of 2,937 cm^{-1}, while C=O and O-H groups associated with carboxyl and phenolic components are observed at peaks of 1,643 and 1,530 cm^{-1}. Additionally, the N-H group is identified at the peak of 1,370 cm^{-1}. The C-OH band vibration is observed at a wavenumber of 1,025 cm^{-1}, and the C-N-S shift originating from the polypeptide structure is identified at the peak of 525 cm^{-1} [20]. Examples of peaks that have diminished include those at 3,400, 2,937, 1,643, 1,025, and 525 cm^{-1}, indicating a reduction in hydroxyl functional groups originating from water content or N-H phenolic groups. This suggests that the hydrochar synthesis process was successful [21].

Surface area BET analysis

The hysteresis curves of Spi and SpiHC materials exhibit type IV(a) isotherm behavior, as shown in **Figure 1(c)**. Materials with type IV(a) isotherm curves typically have pore sizes in the mesoporous range (2 nm $\leq$ d $\leq$ 50 nm), which influence the adsorption and desorption of gases [22], [23]. **Table 1** reveals that the surface area of SpiHC has increased significantly to 5.369 m^2/g, compared to the initial surface area of 0.203 m^2/g for Spi. This enhanced surface area indicates greater potential for more effective adsorption.

Table 1 BET Analysis of Spi and SpiHC.

Material	S_{BET} (m^2/g)	Average pore size (nm)	Average pore volume (cm^3/g)
Spi	0.203	88	2.7
SpiHC	5.369	4.88	0.013

Selectivity study

The deconvolution of absorbance spectra of anionic dye selectivity before and after adsorption can be seen at **Figure 2**. Based on the data in **Table 2**, Direct Yellow (DY) showed the highest adsorption percentage compared to other anionic dyes, both on *Spirogyra* sp. (Spi) and hydrochar material (SpiHC), at 54.02 and 62.07 %, respectively. This indicates that DY is the most selective dye to both materials, with a significant increase in adsorption efficiency after becoming SpiHC. This selectivity could be due to the compatibility of the chemical properties of DY with the active groups present on the adsorbent surface, especially after being made into hydrochar.

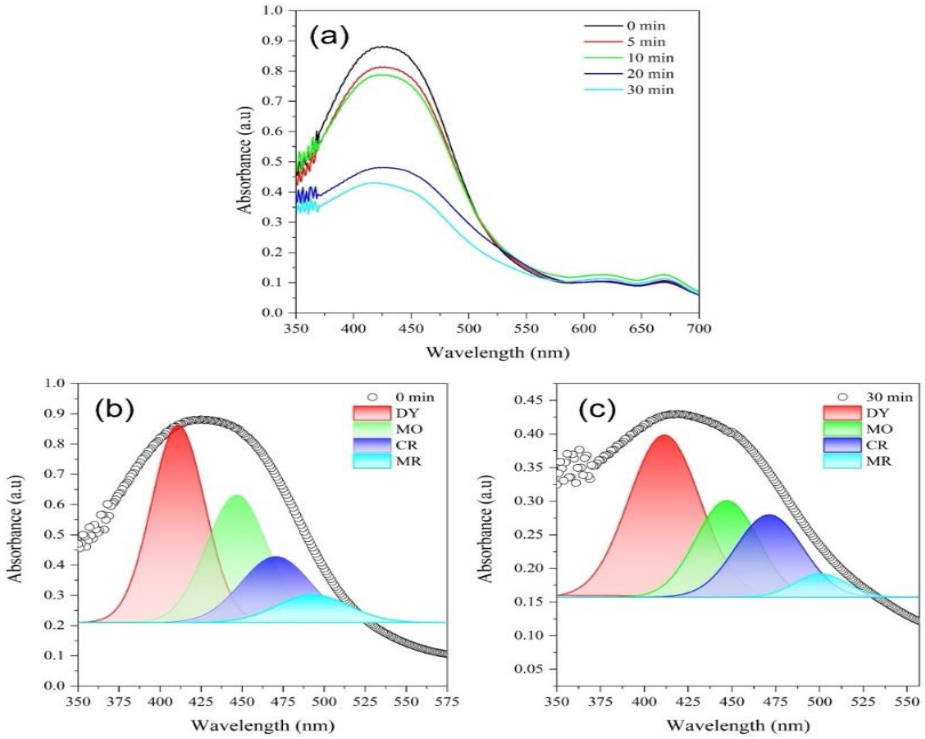

Figure 2 Deconvolution Curves of Adsorption to Anionic Dyes Initial Concentration (a), Adsorption by Spi (b) and SpiHC (c) Materials.

Table 2 The Percentage Adsorption Anionic Dye Selectivity by Spi and SpiHC.

Dyes	Adsorption (%)	
	Spi	SpiHC
DY	54.02	62.07
MO	53.13	53.13
CR	36.36	40.91
MR	38.71	29.03

Adsorption study

The pHpzc (point of zero charge), illustrated in **Figure 3(a)**, represents the pH at which the material is electrically neutral, such as an adsorbent with a characteristic surface charge. In adsorption processes, pHpzc is closely related to the adsorbate being utilized. When the pHpzc of a material is below the optimum pH for adsorption, the surface is positively charged; conversely, if the pHpzc is above the optimum pH, the surface becomes negatively charged [24]. The pHpzc values for Spi and SpiHC materials are 6.7 and 6.48, respectively. As shown in **Figure 3(b)**, the optimal adsorption conditions direct yellow on Spi and SpiHC materials occur at a pH of 6, which is below their pHpzc. On these conditions, the materials exhibit positif surface charges.

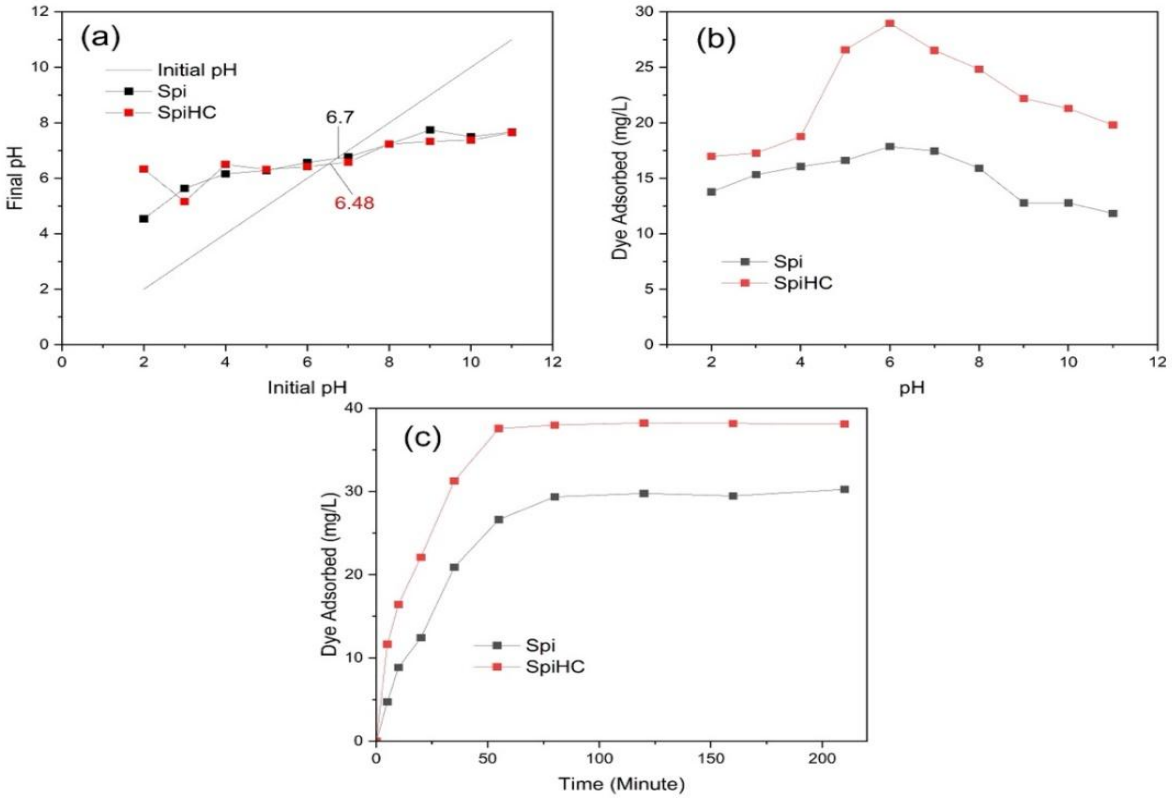

Figure 3 The pHpzc (a), pH Adsorption (b) and Time Adsorption (c) of Spi and SpiHC.

Table 3 shows the adsorption kinetics parameters using the first-order (PFO) and second-order (PSO) models for the adsorbents *Spirogyra sp.* (Spi) and hydrocarbon-treated (SpiHC) material. For the Spi adsorbent, the PFO model gives a Qe calc of 29.778 mg/g, which is close to Qe exp (29.353 mg/g) with a coefficient of determination R2 = 0.9791, indicating a good fit, although the rate constant k1 is relatively low (0.034 min^{-1}). In contrast, the PSO model shows a higher Qe calc (33.670 mg/g) with R2 = 0.981, indicating a better fit compared to the PFO model for the Spi adsorbent. For the SpiHC adsorbent, the PFO model gives Qe calc = 25.651 mg/g with R2 = 0.9979, while the PSO model gives Qe calc = 28.249 mg/g with R2 = 0.992. Although the PFO model provides a slightly higher R2, the PSO model shows a better fit with a Qe calc value that is closer to Qe exp (37.562 mg/g). Overall, the PSO model is more suitable for describing the adsorption kinetics for both adsorbents.

Table 3 The Kinetic Parameters PFO and PSO models of Spi and SpiHC.

Adsorbent	Qe exp (mg/g)	PFO			PSO		
		Qe calc (mg/g)	k_1 (min^{-1})	R^2	Qe calc (mg/g)	k_2 (g/mg)/min	R^2
Spi	29.353	29.778	0.034	0.9791	33.670	0.001	0.981
SpiHC	37.562	25.651	0.042	0.9979	28.249	0.003	0.992

Based on the data presented in **Table 4**, the adsorption isotherms for both adsorbents, Spi and SpiHC, were analyzed using the Langmuir and Freundlich models. The Langmuir parameters indicate that the maximum adsorption capacity (Qmax) for Spi shows a decreasing trend with increasing temperature, from 90.91 mg/g at 30 °C to 45.45 mg/g at 60 °C. This suggests that adsorption on Spi is exothermic, where higher temperatures reduce the interaction between the adsorbent and the adsorbate. Conversely, SpiHC exhibits fluctuating Qmax values, with the highest value of 95.24 mg/g at 40 °C. This indicates that the modification to hydrochar enhances the adsorption capacity at specific temperatures. The Langmuir coefficient (kL) parameters show relatively small values for both adsorbents, indicating low surface affinity for the adsorbate. The R^2 values for the Langmuir model for both adsorbents are below 0.9, suggesting that this model is less suitable for describing the adsorption process. In contrast, the Freundlich model provides a better fit, as evidenced by the high R^2 values ($\geq$ 0.97) under all conditions. The Freundlich exponent (n) for Spi is above 1 at all temperatures, indicating that the adsorption is more heterogeneous with strong adsorbate binding. For SpiHC, the n values reflect weaker adsorption characteristics compared to Spi, with values below 1 at 30 °C but close to 1 at other temperatures. The Freundlich capacity (kF) values for SpiHC tend to be higher than those for Spi, suggesting that the modification to hydrochar enhances surface affinity for the adsorbate.

Table 4 The Adsorption Isotherm Langmuir and Freundlich Parameter of Spi and SpiHC.

Adsorbent	T (°C)	Langmuir			Freundlich		
		Qmax	kL	R^2	n	kF	R^2
Spi	30	90.91	0.015	0.737	0.859	1.131	0.997
	40	50	0.061	0.893	1.472	3.827	0.981
	50	53.76	0.058	0.845	1.483	4.049	0.987
	60	45.45	0.077	0.855	1.628	4.620	0.985
SpiHC	30	64.52	0.067	0.794	0.600	3.998	0.972
	40	95.24	0.052	0.799	0.830	4.798	0.995
	50	73.53	0.069	0.748	0.791	4.901	0.988
	60	70.92	0.069	0.692	0.785	4.690	0.983

Based on the thermodynamic adsorption data for Spi and SpiHC at **Table 5**, the ΔH values indicate that the adsorption process for both adsorbents is endothermic, with ΔH values of 6.679 kJ/mol for Spi and 2.820 kJ/mol for SpiHC. This suggests that energy is required for adsorption to occur, which may be related to the rearrangement of water molecules around the adsorbent or specific interactions between the adsorbent and adsorbate. The positive ΔS values for both adsorbents (0.028 kJ/mol for Spi and 0.024 kJ/mol for SpiHC) indicate an increase in system randomness after adsorption. This can be attributed to the release of bound water molecules from the adsorbent surface or the restructuring of the adsorbate during the adsorption

process. The negative ΔG values at all tested temperatures indicate that adsorption occurs spontaneously. For Spi, the ΔG values become more negative with increasing temperature (from –1.67 kJ/mol at 30 °C to –2.50 kJ/mol at 60 °C), suggesting that higher temperatures enhance the spontaneity of the adsorption process. A similar trend is observed for SpiHC, with ΔG values ranging from –4.49 to –5.21 kJ/mol. The more negative ΔG values for SpiHC compared to Spi indicate that SpiHC has a higher adsorption affinity for the adsorbate at the same concentration.

Table 5 The Adsorption Thermodynamic Parameter of Spi and SpiHC.

Adsorbent	Concentration (mg/L)	ΔH (kJ/mol)	ΔS (kJ/mol)	ΔG (kJ/mol)			
				30 °C	40 °C	50 °C	60 °C
Spi	20	6.679	0.028	–1.67	–1.94	–2.22	–2.50
SpiHC	20	2.820	0.024	–4.49	–4.73	–4.97	–5.21

Regeneration cycles

Figure 4 show the regeneration cycle of material. SpiHC demonstrates superior regeneration performance compared to Spi, particularly in maintaining adsorption efficiency up to the fourth cycle. In the second cycle, the adsorption efficiencies of Spi and SpiHC were 47.77 and 85.74 %, respectively. Meanwhile, in the fourth cycle, Spi's efficiency drastically declined to 30.55 %, whereas SpiHC was still able to maintain an efficiency of 67.11 %. This indicates that SpiHC possesses a more stable structure or surface properties that are more resistant to degradation during the regeneration process. Conversely, Spi experienced a significant decrease in efficiency after the second cycle, highlighting the material's limited stability for reuse. Therefore, SpiHC has an advantage in regeneration applications for at least 4 cycles, compared to Spi, which is effective only up to 2 cycles.

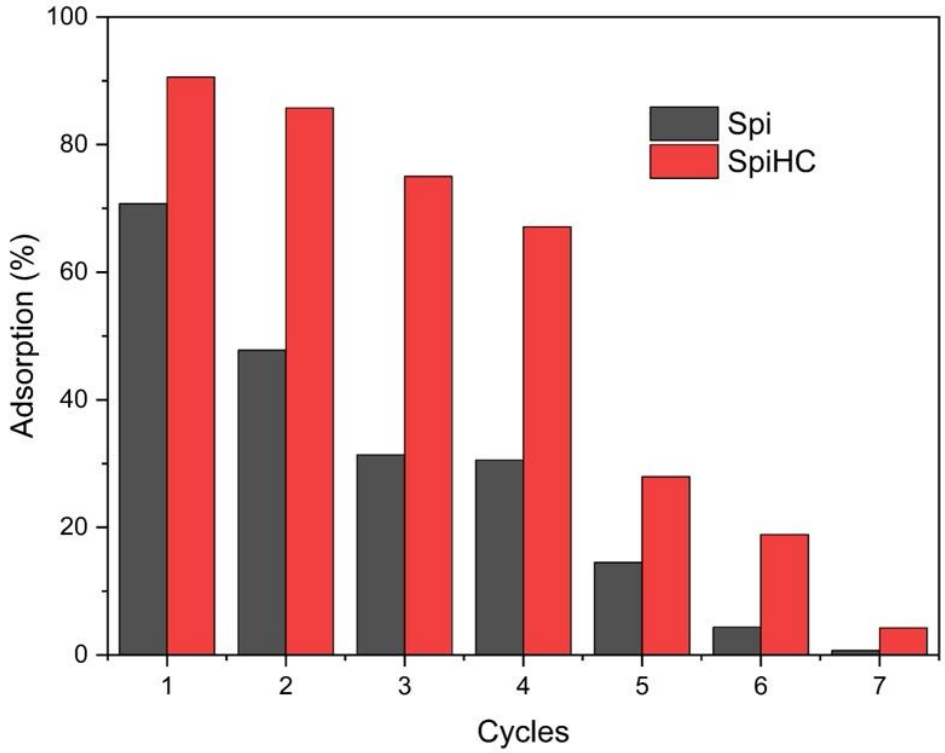

Figure 4 The Graphic Regeneration Cycle of Spi and SpiHC.

Comparison of Spi and SpiHC ability with other materials on DY adsorption

The materials investigated in this study, Spi and SpiHC, demonstrate superior performance compared to other materials previously reported for the adsorption of DY dye. The comparison data of the materials in this study with other materials on the adsorption of DY is shown in **Table 6**. Spi and SpiHC exhibit a higher maximum adsorption capacity, which indicates their ability to adsorb a greater amount of dye per unit mass of the material. Additionally, these materials possess excellent regeneration capabilities, allowing for multiple cycles of adsorption-desorption with minimal loss in efficiency. This feature is critical for sustainable wastewater treatment processes.

The remarkable adsorption capacity and reusability of Spi and SpiHC highlight their effectiveness as adsorbents for the removal of anionic dyes like Direct Yellow. These characteristics make them promising candidates for practical applications in environmental remediation, particularly in addressing dye pollution in aqueous solutions.

Table 6 comparison data of spi and spiHC with other materials on DY adsorption

Materials	Adsorption Capacity (mg/g)	Optimum pH	Regeneration Cycle	References
Biomass-derived porous graphitic activated carbon	42.02	2	5 (77 %)	[25]
Organobentonite-surfactant octadecyl amine-ethanol	108.696	7	3 (40.38 %)	[26]
Nano bentonite	250	3	-	[27]
Zeolite	83.3	3	-	[28]
Modified Graphene Oxide	10.71	-	-	[29]
Polyethyleneimine treated	65.8	2	-	[30]
Cotton Fiber	83.179	7	-	[31]
Modified Pumice	1.22	6	-	[32]
Spi	90.91	6	2 (47.77 %)	This study
SpiHC	95.24	6	4 (67.11 %)	This study

The adsorption performance of Spi and SpiHC was compared with various adsorbents reported in the literature, as summarized in **Table 6**. SpiHC exhibited a maximum adsorption capacity of 95.24 mg/g, which is higher than several other adsorbents, such as modified graphene oxide (10.71 mg/g) Azizi *et al.* [29], polyethyleneimine-treated adsorbents (65.8 mg/g) Sadaf *et al.* [30], and zeolite (83.3 mg/g) [28]. While nano bentonite demonstrated a higher adsorption capacity of 250 mg/g [27], its regeneration ability was not reported, making it difficult to assess its long-term applicability. In contrast, SpiHC maintained a notable regeneration capacity, retaining 67.11 % efficiency after 4 cycles, outperforming organobentonite (40.38 % after 3 cycles) Hakim *et al.* [26] and biomass-derived activated carbon (77 % after 5 cycles) [25].

Additionally, Spi and SpiHC exhibit optimal adsorption at pH 6, which differs from other adsorbents such as biomass-derived activated carbon (pH 2) Reddy *et al.* [25] and nano bentonite (pH 3) [27]. This moderate pH requirement makes Spi and SpiHC more suitable for practical wastewater treatment applications, as extreme pH conditions may require additional chemical adjustments. The combination of high adsorption capacity, good regeneration ability, and favorable pH conditions highlights the potential of Spi and SpiHC as effective and sustainable adsorbents for dye removal in aqueous solutions.

Conclusions

This study successfully synthesized hydrochar (SpiHC) from *Spirogyra* sp. algae biomass using a hydrothermal method. Characterization results indicated

significant improvements in the material properties of SpiHC, including increased surface area and enhanced structural organization, compared to raw *Spirogyra* sp. (Spi). The adsorption selectivity study demonstrated that SpiHC exhibited the highest efficiency for direct yellow (DY) dye, with 62.07 % adsorption compared to 54.02 % for Spi. Adsorption experiments confirmed that SpiHC performed optimally at pH 6, aligning well with the pseudo-second-order kinetic model and Freundlich isotherm, indicating its heterogeneous adsorption behavior. Thermodynamic analysis showed that the adsorption process was endothermic, spontaneous, and more favorable for SpiHC, with higher adsorption affinity than Spi. Furthermore, SpiHC retained 67.11 % adsorption efficiency after 4 regeneration cycles, demonstrating its superior stability and reusability for water treatment applications. These findings highlight the potential of *Spirogyra*-derived hydrochar as an eco-friendly and cost-effective adsorbent for addressing wastewater challenges. Future research should focus on scaling up the synthesis process, optimizing adsorption conditions for different pollutants, and evaluating the economic feasibility of SpiHC in real-world applications.

Acknowledgements

Thank you for Research Center of Inorganic Materials and Coordination Complexes Universitas Sriwijaya, Indonesia to support this research.

References

[1] S Wibiyan, I Royani, and A Lesbani. Selective adsorption of cationic and anionic dyes using Ni/Al layered double hydroxide modified with *Eucheuma cottonii*. *Indonesian Journal of Material Research* 2024; **2(1)**, 1–6.

[2] M Zabihi and A Motavalizadehkakhky. PbS/ZIF-67 nanocomposite: Novel material for photocatalytic degradation of basic yellow 28 and direct blue 199 dyes. *Journal of the Taiwan Institute of Chemical Engineers* 2022; **140**, 104572.

[3] S. Yao, M Fabbricino, L Pontoni, M Race, F Parrino, L Savignano, G D'Errico and Y Chen. Characterization of anthropogenic organic matter and its interaction with direct yellow 27 in wastewater: Experimental results and perspectives of resource recovery. *Chemosphere* 2022; **286**, 131528.

[4] F Ullah, G Ji, M Irfan, Y Gao, F Shafiq, Y Sun, QU Ain and A Li. Adsorption performance and mechanism of cationic and anionic dyes by KOH activated biochar derived from medical waste pyrolysis. *Environmental Pollution* 2022; **314**, 120271.

[5] C Cui, W Qiao, D Li and L Wang. Dual cross-linked magnetic gelatin/carboxymethyl cellulose cryogels for enhanced Congo red adsorption: Experimental studies and machine learning modelling. *Journal of Colloid and Interface Science* 2025; **678**, 619-635.

[6] P Doondani, D Panda, V Gomase, KR Peta and R Jugade. Novel Chitosan-ZnO nanocomposites derived from Nymphaeaceae fronds for highly efficient removal of reactive blue 19, reactive orange 16, and congo red dyes. *Environmental Research* 2024; **247**, 118228.

[7] YAB Neolaka, ZS Ngara, Y Lawa, JN Naat, DP Benu, A Chetouani, H Elmsellem, H Darmokoesoemo and HS Kusuma. Simple design and preliminary evaluation of continuous submerged solid small-scale laboratory photoreactor (CS4PR) using TiO2/NO3-@TC for dye degradation. *Journal of Environmental Chemical Engineering* 2019; **7(6)**, 103482.

[8] EA Alabbad. Efficacy assessment of natural zeolite containing wastewater on the adsorption behaviour of Direct Yellow 50 from; equilibrium, kinetics and thermodynamic studies. *Arabian Journal of Chemistry* 2021; **14(4)**, 10301.

[9] GM Ibrahim, SM Alshahrani, EH Alosaimi, WA Alshahrani, B El-Gammal, A Fawzy, N Alqarni, H Elhouichet and HM Safaa. Adsorption mechanism elucidation of anionic congo red onto modified magnetic nanoparticle structures by quantum chemical and molecular dynamics. *Journal of Molecular Structure* 220224; **1298**, 136992.

[10] N Ahmad, FS Arsyad, I Royani and A Lesbani. Selectivity of malachite green on cationic dye mixtures toward adsorption on magnetite humic acid. *Environment and Natural Resources Journal* 2022; **20(6)**, 634-643.

[11] NR Palapa, N Yuliasari, PMSBN Siregar, A Wijaya, A Amri, N Ahmad and A Lesbani.

Selective adsorption of direct group anionic dyes on layered double hydroxide-chitosan composites. *Bulletin of Chemical Reaction Engineering and Catalysis* 2023; **18(1)**, 37-47.

[12] Y Achour, L Bahsis, EH Ablouh, H Yazid, MR Laamari and ME Haddad. Insight into adsorption mechanism of congo red dye onto bombax buonopozense bark activated-carbon using Central composite design and DFT studies. *Surfaces and Interfaces* 2021; **23**, 100977.

[13] VA Tran, KB Vu, TT Vo, VT Le, HH Do, LG Bach and S Lee. Experimental and computational investigation on interaction mechanism of Rhodamine B adsorption and photodegradation by zeolite imidazole frameworks-8. *Applied Surface Science* 2021; **538**, 148065.

[14] N Normah, N Juleanti, NR Palapa, T Taher, PMSBN Siregar, A Wijaya and A Lesbani. Hydrothermal carbonization of rambutan peel (Nephelium lappaceum L.) as a green and low-cost adsorbent for Fe(II) removal from aqueous solutions. *Chemistry and Ecology* 2022; **38(3)**, 284-300.

[15] X Luo, Z Huang, J Lin, X Li, J Qiu, J Liu and X Mao. Hydrothermal carbonization of sewage sludge and in-situ preparation of hydrochar/MgAl-layered double hydroxides composites for adsorption of Pb(II). *Journal of Cleaner Production* 2020; **258**, 120991.

[16] MA Khalaf. Biosorption of reactive dye from textile wastewater by non-viable biomass of Aspergillus niger and *Spirogyra* sp. *Bioresource Technology* 2008; **99(14)**, 6631-6634.

[17] Normah, NR Palapa, T Taher, R Mohadi, FS Arsyad, A Priambodo and A Lesbani. Competitive removal of cationic dye using nial-ldh modified with hydrochar. *Ecological Engineering and Environmental Technology* 2021; **22(4)**, 124-135.

[18] M Hasanah, N Normah, A Wijaya, FS Arsad, R Mohadi and A Lesbani. High selectivity and adsorption capacity for congo red toward anionic dyes by adsorbent: Modified LDH with hydrochar made from Nephelium Lappaceum Peel. *Global Nest Journal* 2022; **24(3)**, 487-494.

[19] N Juleanti, N Normah, PMSBN Siregar, A Wijaya, NR Palapa, T Taher, N Hidayati, R Mohadi and A Lesbani. Comparison of the adsorption ability of MgAl-HC, CaAl-HC, and ZaAl-hc composite materials based on duku peel hydrochar in adsorption of direct green anionic dyes. *Indonesian Journal of Chemistry* 2022; **22(1)**, 192-204.

[20] Z Djezzar, A Aidi, H Rehali, S Ziad and T Othmane. Characterization of activated carbon produced from the green algae *Spirogyra* used as a cost-effective adsorbent for enhanced removal of copper(ii): Application in industrial wastewater treatment. *RSC Advances* 202; **14(8)**, 5276-5289.

[21] A Aksu, N Kutuk, O Caylak, E Kasaka, S Cetinkaya, MM Maslov and S Kaya. *Theoretically supported experimental analyses on Safranin O biosorption from textile wastewater via dead biomass of Spirogyra porticalis*. Springer Nature, New York, 2024.

[22] A. Lesbani, N Ahmad, R Mohadi, I Royani, S Wibiyan, Amri and Y Hanifah. Selective adsorption of cationic dyes by layered double hydroxide with assist algae (Spirulina platensis) to enrich functional groups. *JCIS Open* 2024; **15**, 100118.

[23] N Gibson, P Kuchenbecker, K Rasmussen, VD Hodoroaba and H Rauscher. *Volume-specific surface area by gas adsorption analysis with the BET method*. Elsevier Science, Amsterdam, Netherlands, 2019.

[24] W Li, E Tao, X Hao, N Li, Y Li and S Yang. MMT and ZrO2 jointly regulate the pore size of graphene oxide-based composite aerogel materials to improve the selective removal ability of Cu(II). *Separation and Purification Technology* 2024; **331**, 125506.

[25] N Smjecanin, D Buzu, E Masic, M Nuhanovvic, J Sulejmanovic, O Azhar and F Sher. Algae based green biocomposites for uranium removal from wastewater: Kinetic, equilibrium and thermodynamic studies. *Materials Chemistry and Physics* 2022; **283**, 125998.

[26] YS Reddy, TJ Jose, BDR Naresh, KP Sampath and KK Kaviyarasu. Equilibrium, kinetic, and thermodynamic study of Direct Yellow 12 dye adsorption by biomass - derived porous graphitic activated carbon. *Biomass Conversion and Biorefinery* 2025; **15**, 6817-6833.

[27] YM Hakim, Mardiyanto, I Royani and R Mohadi. Organobentonite fabrication assisted by surfactant octadecylamine intercalation under hydrothermal/solvothermal condition for effective direct yellow dye removal. *Kuwait Journal of Science* 2024; **51(6)**, 100292.

[28] AS Mahmoud. Effect of nano bentonite on direct yellow 50 dye removal; Adsorption isotherm, kinetic analysis, and thermodynamic behavior. *Progress in Reaction Kinetics and Mechanism* 2022; **47(1)**, 14686783221090377.

[29] EA Alabbad. Effect of direct yellow 50 removal from an aqueous solution using nano bentonite; adsorption isotherm, kinetic analysis and also thermodynamic behavior. *Arabian Journal of Chemistry* 2023; **16(2)**, 104517.

[30] A Azizi, E Moniri, AH Hassani, HA Panahi and M Jafarinezhad. Nonlinear and linear analysis of direct yellow 50 adsorption onto modified graphene oxide: Kinetic, isotherm, and thermodynamic studies. *Desalination and Water Treatment* 2021; **229**, 352-361.

[31] S Sadaf, HN Bhatti, S Nausheen and M Amin. Application of a novel lignocellulosic biomaterial for the removal of Direct Yellow 50 dye from aqueous solution: Batch and column study. *Journal of the Taiwan Institute of Chemical Engineers* 2015; **47**, 160-170.

[32] LFM Ismail, HB Sallam, SAA Farha, AM Gamal and GEA Mahmoud. Adsorption behaviour of direct yellow 50 onto cotton fiber: Equilibrium, kinetic and thermodynamic profile. *Spectrochimica Acta Part A: Molecular and Biomolecular Spectroscopy* 2024; **131**, 657-666.

[33] M Ahmadian, N Yousefi and A Toolabi. Adsorption of direct yellow 9 and acid orange 7 from aqueous solutions by modified pumice. *Asian Journal of Chemistry* 2012; **24(7)**, 3094-3098.